EFFECT OF GRAIN SIZE ON MECHANICAL PROPERTIES OF 3Y-TZP CERAMICS

MARTIN TRUNEC

Department of Ceramics and Polymers, Brno University of Technology
Technicka 2896/2, 616 69 Brno, Czech Republic

E-mail: trunec@fme.vutbr.cz

The dependence of mechanical properties of 3Y-TZP ceramics on their grain sizes in the range from 0.19 μm to 2.15 μm has been investigated. Vickers indentation tests were used to determine hardness and fracture toughness. The hardness decreased with increasing grain size. The fracture toughness was almost constant for ceramics with the grain size up to 0.40 μm and then grew with increasing grain size up to 7.8 MPam$^{0.5}$ for ceramics with grain size of 1.8 μm. Above this grain size a spontaneous transformation from tetragonal to monoclinic phase occurred. Ceramic samples with grain sizes of 0.30 μm and 0.78 μm yielded similar bending strength, 1020 and 1011 MPa, respectively. The microstructural coarsening required for achieving larger grain size resulted in a higher scatter of strength values, which was demonstrated by a lower Weibull modulus (13.0 vs. 7.54). The mechanical properties of nanocrystalline 3Y-zirconia ceramics coarsened to the grain size range from 0.085 to 0.70 μm were also investigated and compared. Differences in mechanical behaviour of investigated ceramics were observed and their possible causes discussed.

INTRODUCTION

Yttria-stabilized tetragonal zirconia polycrystals (Y-TZP) have proved to be important structural ceramics. High strength and fracture toughness make them attractive candidates for a number of demanding applications. It was established that these advantageous properties are strongly influenced by the ceramic microstructure [1]. The relationships between microstructure and mechanical properties in Y-TZP ceramics have been studied extensively over the past two decades. It is now generally agreed that the transformation toughening effect (stress-induced tetragonal to monoclinic phase transformation) in Y-TZP ceramics is grain size dependent [2 7]. The larger the tetragonal grains the greater propensity to undergo stress-induced transformation to an equilibrium structure, resulting in an enhanced toughness. The maximum toughness lies near the critical grain size, where the tetragonal grains undergo spontaneous tetragonal to monoclinic transformation [7]. It was found that this critical grain size depends on the yttria content [6, 7]. However, the critical grain size, cited for 3Y-TZP (3 mol% Y_2O_3), which is the most common zirconia ceramic material, varies significantly (from 1 to 6 μm) [3, 8-9]. This could be attributed to different processing procedures that result in different ceramic microstructures. Thus, microstructural parameters like porosity, grain size distribution, yttrium distribution in grains, purity, phase assemblage, etc. need to be taken into account for evaluating the microstructure.

In contrast to the fracture toughness the strength of 3Y-TZP reaches its maximum usually at smaller grain size [5, 10]. Increasing size of failure origin coupled with microstructural coarsening was identified as the reason for strength decrease in ceramics with large grains [11]. However, the increase of strength with decreasing grain size cannot be extended to the nanocrystalline range in 3Y-TZP. Eichler et al. [10] determined the strength maximum for 3Y-TZP in the submicron range and noted a clear strength decrease in the nanocrystalline grain size range (~100 nm). In this case, the strength decrease was attributed to the grain size dependence of fracture toughness. A decrease in the fracture toughness was observed as the grain size changed from the submicrometre to the nanometre range [10, 12]. These results validate the assumption that the increase of critical defects during microstructural coarsening is connected with the formation of stress induced transformed regions at the free surface and takes place preferentially in ceramics with grains near the critical size [11]. Nevertheless, special processing of TZP ceramics has been reported, which can partially eliminate the increase of critical defects during coarsening, resulting in almost constant strength, independent of grain size [8, 9].

The objective of the present investigation was to describe the dependence of mechanical properties of commercial submicrometre-grained 3Y-TZP ceramics on grain size and to compare their mechanical properties to the mechanical properties of nanocrystalline zirconia ceramics and nanocrystalline ceramics coarsened to the submicrometre range.

EXPERIMENTAL

Two zirconia powders stabilized by 3 mol% Y_2O_3 were used for the preparation of test specimens. Commercial zirconia powder TZ-3YB (Tosoh, Japan) was cold isostatically pressed at 300 MPa into disk-shaped bodies (diameter 28 mm; thickness 5 mm). For comparison, a nanocrystalline zirconia powder B261 (BUT, Czech Republic) was used. Details of the preparation of the nanopowder can be found in [13]. Nanocrystalline powder was cold isostatically pressed at 1000 MPa without additives. The pressed bodies were 18 mm in diameter and 5 mm thick. These bodies were ground to a thickness of 1.5 mm prior to sintering. Both types of bodies were densified by pressureless sintering in air at temperatures from 1100 to 1650°C and dwell times ranging from 0 to 50 hours.

The density of sintered specimens was determined by the Archimedes method [14] with distilled water as the immersing medium. The relative density of all ceramic bodies was calculated using the value 6.1 g·cm⁻³ for the theoretical density of 3Y-TZP. The grain size of the sintered ceramics was evaluated by linear intercept method (without correction) on scanning electron microscopy (SEM) micrographs of polished and thermally etched samples, in a similar way as in [15]. At least three micrographs and total of 300 intersects were evaluated to determine the average grain size for each sintering batch. The phase composition of the sintered ceramics was determined by X-ray diffraction (XRD) analysis (X´pert, Philips, the Netherlands). The X-ray spectra of polished and fracture surface were obtained and the phase content was quantified using Rietveld analysis.

For hardness and fracture toughness evaluation Vickers indentation tests (LV 700, Leco, USA) were used. Prior to indentation ceramic disks were mounted in a resin and their surfaces ground and polished (finishing with 1 µm diamond polishing fluid). Hardness tests were performed at a load of 9.8 N (1 kg) and a hold of 15 s. For determining the Vickers hardness, HV (MPa), the following expression was used:

$$HV = 1.8544 \, P/d^2, \qquad (1)$$

where P is the applied load and d is the average diagonal line length of the indentation. Ten indentations were

made for each sample. Toughness was calculated directly from the crack lengths produced by Vickers indentation at higher loads. Applied loads were 49.05 N (5 kg), 98.1 N (10 kg), 196.2 N (20 kg) and 294.3 N (30 kg) always with a hold of 15 s. The crack lengths were measured immediately after indentation using a calibrated optical microscope. The fracture toughness, K_{Ic} (MPam⁰·⁵), was calculated using the equation given by Niihara et al. [16] for Palmqvist cracks:

$$K_{Ic} = 9.052 \times 10^{-3} \, H^{3/5} \, E^{2/5} \, d \, c^{-1/2} , \qquad (2)$$

where H is the hardness, E the Young modulus (a value of 210 GPa has been assumed for all the samples), d is the average diagonal line length of the indentation and c is the length of the Palmqvist crack. Ten valid measurements were determined for each sample. The valid measurements had to satisfy the requirements of the JIS R 1607 [17] on acceptable indentation cracks.

The flexural strength was determined for selected ceramic samples in four-point bending at a crosshead speed of 2 mm/min, using fully articulated fixture with a 10 mm inner and 20 mm outer span (in the "A" arrangement according to the EN 843-1 [18]). Ceramic bars with dimensions ca. $2.5 \times 2 \times 25$ mm³ were cut from the disks, ground and polished (finally with 1-2 µm grained diamond paste). The parameters of the Weibull strength distribution were calculated numerically, in compliance with the ENV 843-5 [19].

RESULTS AND DISCUSSION

Microstructure and phase analysis

Various sintering schedules were applied to zirconia green bodies to obtain dense sintered ceramics with different grain sizes. Only those sintering schedules that resulted in sintered densities exceeding 99% of theoretical density (% t.d.) were employed.

A temperature of 1400°C was the lowest temperature used in sintering the TZ-3YB ceramics; this was necessary to obtain a dense sintered body. Larger grains were obtained by the action of both higher sintering temperatures and longer sintering times. Sintering schedules and resulting densities and grain sizes are shown in Table 1. The density of sintered TZ-3YB bodies was constant up to the sintering temperature of 1650°C. At the sintering temperature of 1650°C the density of TZ-3YB ceramics decreased with increasing sintering time. The structure of ceramics remained dense but the theoretical density of these ceramics decreased due to spontaneous transformation of the tetragonal into the monoclinic phase (see Table 1). The average grain size of TZ-3YB ceramics ranged from 0.19 µm (sintered at 1400°C/2 h) to 2.15 µm (sintered at 1650°C/50 h). The

critical grain size for spontaneous transformation from tetragonal to monoclinic phase lies between 1.8 and 2.15 μm, where the content of monoclinic phase in TZ 3YB ceramics increased dramatically. The sample sintered at 1650°C for 50 hours consisted of 77 % monoclinic phase and was severely cracked due to volume changes accompanying $t \rightarrow m$ transformation. Mechanical properties could not be determined for these ceramics. Several authors [8, 9, 11] have found large cubic grains in thermally treated 3Y-TZP samples. In our case no exaggerated grain growth was observed during the microstructural coarsening.

The zirconia nanopowder B261 could be sintered to dense bulk ceramics already at the temperature of 1100°C and dwell time of 4 hours. The microstructure remained nanoscaled with an average grain size of 85 nm. Microstructural coarsening occurred at higher sintering temperatures. However, the grain growth kinetics of B261 ceramics was different from that in TZ 3YB ceramics. B261 ceramics sintered at 1550°C/5 h had larger grains than TZ 3YB ceramics sintered under the same conditions (0.70 vs. 0.48 μm). Moreover, the density of B261 ceramics decreased sharply already at small grain sizes where no monoclinic phase was detected. Figure 1 shows the density as a function of grain size for both TZ-3YB and B261 ceramics. The reason for the density change in B261 ceramics is not completely clear. According to the equilibrium phase diagram given by Scott [20] the maximum amount of cubic phase occurring in 3 mol% Y_2O_3–ZrO_2 ceramics sintered at 1550°C can be about 28 %. Matsui et al. [21] showed that in tetragonal zirconia ceramics similar to TZ-3YB the Y^{3+} ions segregated at grain boundaries over a width of ~10 nm. Consequently, the cubic phase

started to form from grain boundaries and a triple junction, at which Y^{3+} ions were segregated. A mixed tetragonal-cubic structure was confirmed in TZ-3YB ceramics by XRD analysis. In B261 ceramics the nanocrystalline structure probably allowed other mechanisms of phase structure development to take place that resulted in the one-phase tetragonal structure. This fact could explain the faster grain growth found in B261 ceramics. Typical microstructures of TZ-3YB ceramics are shown in Figures 2-4 and microstructures of B261 ceramics are shown in Figures 5 and 6. The holes and voids visible in micrographs on Figures 4 and 6 are believed not to be pores but rather to result from pulling out the grains during grinding and polishing.
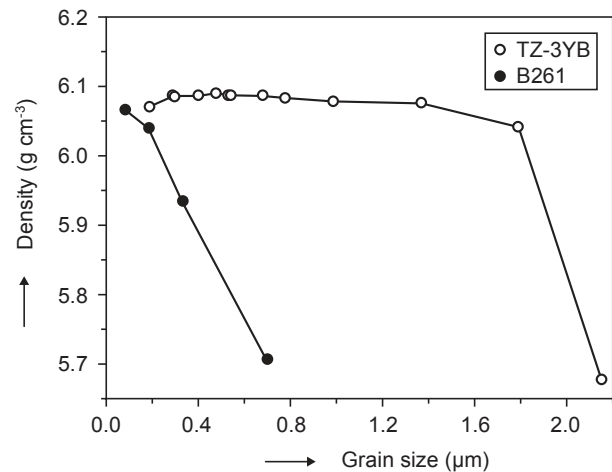

Figure 1. Density of TZ-3YB and B261 ceramics as a function of grain size.

Table 1. Sintering schedules of zirconia ceramics and resulting density, grain size and monoclinic phase content.

Powder/Sample	Sintering schedule (°C)/(h)	Density (g/cm³)	Relative density (% t.d.)	Grain size (μm)	m - ZrO_2 (%)
TZ - 3YB	1400/2	6.07	99.5	0.19	0
TZ - 3YB	1500/2	6.08	99.7	0.30	0
TZ - 3YB	1550/0	6.09	99.8	0.29	0
TZ - 3YB	1550/2	6.09	99.8	0.40	0
TZ - 3YB	1550/5	6.09	99.8	0.48	0
TZ - 3YB	1550/10	6.09	99.8	0.54	0
TZ - 3YB	1600/2	6.09	99.8	0.53	0
TZ - 3YB	1600/5	6.09	99.8	0.68	0
TZ - 3YB	1600/10	6.08	99.7	0.78	0
TZ - 3YB	1650/10	6.08	99.6	0.99	3
TZ - 3YB	1650/20	6.08	99.6	1.37	6
TZ - 3YB	1650/30	6.04	99.1	1.79	13
TZ - 3YB	1650/50	5.68	93.1	2.15	77
B 261	1100/4	6.07	99.4	0.085	0
B 261	1300/6	6.04	99.0	0.19	0
B 261	1450/2	5.93	97.3	0.33	0
B 261	1550/5	5.71	93.6	0.70	0

Mechanical properties

Ten Vickers hardness tests were performed for each ceramic. Average hardness values and their standard deviation are given in Table 2. The hardness of TZ-3YB ceramics clearly decreased with increasing grain size from HV = 12620 MPa at grain size of 0.19 µm to HV = 10971 MPa at grain size of 1.79 µm. The graph in Figure 7 shows the hardness of TZ-3YB ceramics as a function of the inverse square root of grain size. The values in the graph could be reasonably fitted with a line (r^2 = 0.94), which means that this dependence followed the Hall-Petch relationship. The hardness of B261 ceramics showed a higher dispersion but the linear fit seems to be also reasonable. Different parameters of the fits (lower hardness of B261 compared with TZ-3YB ceramics) could be attributed to different phase structure (mixed tetragonal-cubic vs. pure tetragonal).
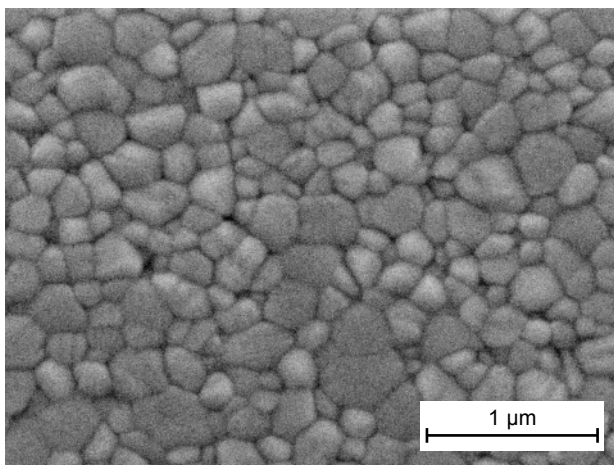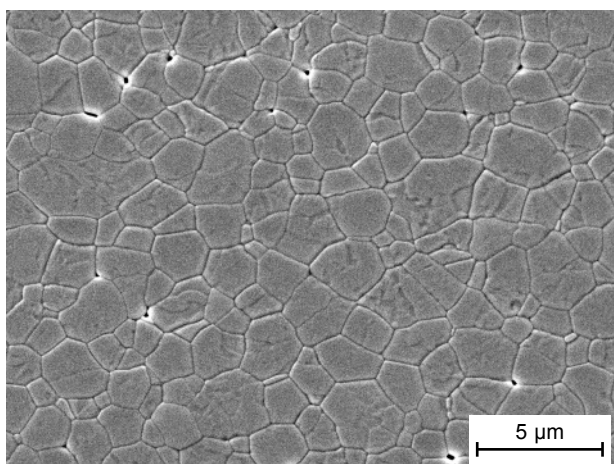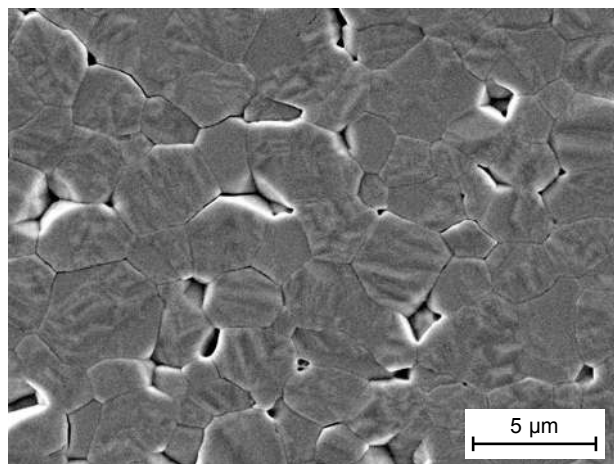

Figure 4. SEM micrograph showing the microstructure of the TZ-3YB ceramics sintered at 1650°C for 50 h.

Figure 2. SEM micrograph showing the microstructure of the TZ-3YB ceramics sintered at 1400°C for 2 h.
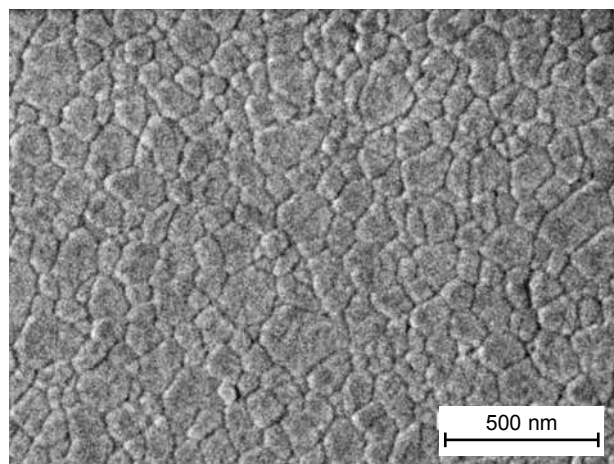

Figure 5. SEM micrograph showing the microstructure of the B261 ceramics sintered at 1100°C for 4 h.

Figure 3. SEM micrograph showing the microstructure of the TZ-3YB ceramics sintered at 1650°C for 20 h.
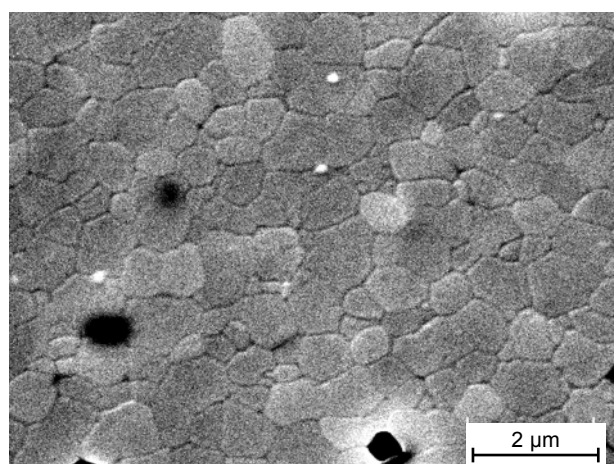

Figure 6. SEM micrograph showing the microstructure of the B261 ceramics sintered at 1550°C for 5 h.

Different loads of Vickers indenter in the range from 49.05 N (5 kg) to 294.3 N (30 kg) were used to generate cracks in ceramic samples. It was verified that in all cases only Palmqvist cracks were produced. Fracture toughness values calculated from crack lengths using Equation (2) at different loads are shown in Table 2. The indenter load of 49.05 N (5 kg) generated unstable cracks that grew further after load release. It was not possible to measure the crack length reliably, therefore the fracture toughness calculated from this load was not included in the Table 2. The graph in Figure 8 shows the dependence of fracture toughness of TZ-3YB ceramics at different loads on grain size. The values of fracture toughness determined at different loads varied significantly. Nevertheless, the dependence of toughness on grain size showed the same trend for all loads. To obtain the most reliable value for the fracture toughness, an average of values determined at different loads was calculated (see Table 2). Figure 9 gives the dependence of the average fracture toughness on grain size for both TZ-3YB and B261 ceramics. This dependence can be divided in two areas. The toughness was almost constant (~ 5.1 MPam$^{0.5}$) up to a grain size of 0.4 μm. In ceramics with larger grains, the toughness increased linearly up to the grain size of 1.8 μm, where the maximum toughness (7.8 MPam$^{0.5}$) was found. Above this grain size spontaneous transformation to the monoclinic phase occurred. Figure 9 shows that both ceramics, TZ-3YB and B261, followed the same toughness dependence on grain size. It also follows from this figure that the transformation toughness effect is grain size dependent only above a particular tetragonal grain size (approx. 0.4 μm).
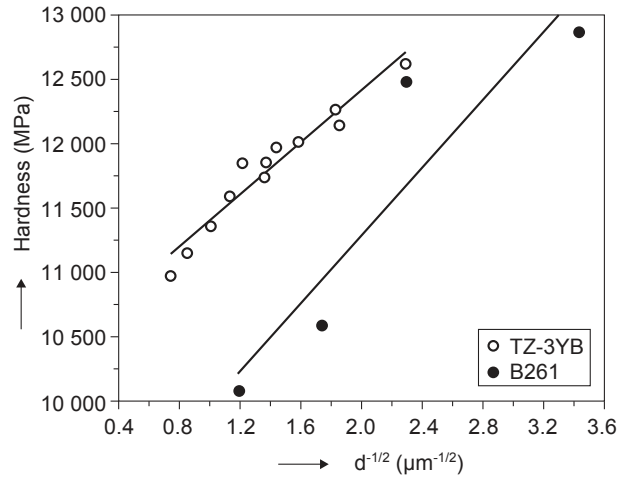

Figure 7. The dependence of the hardness of TZ-3YB and B261 ceramics on the inverse square root of grain size.
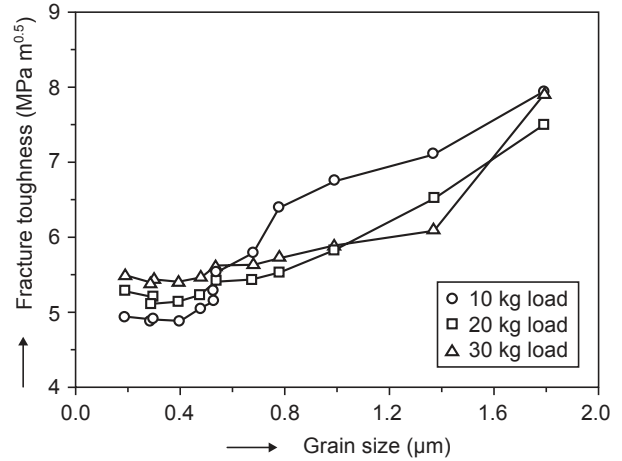

Figure 8. Fracture toughness of TZ-3YB ceramics as a function of grain size determined at different indentation loads.

Table 2. Hardness, *HV*, fracture toughness, K_{Ic}, and their standard deviations, *s*, of zirconia ceramics.

Sample	Sintering schedule (°C)/(h)	Hardness		Fracture toughness						Average
				10 kg		20 kg		30 kg		
		HV	*s*	K_{Ic}	*s*	K_{Ic}	*s*	K_{Ic}	*s*	K_{Ic}
		(MPa)		(MPam$^{0.5}$)						
TZ - 3YB	1400/2	12620	186	4.94	0.07	5.29	0.06	5.49	0.05	5.24
TZ - 3YB	1500/2	12264	135	4.91	0.06	5.20	0.08	5.41	0.05	5.17
TZ - 3YB	1550/0	12137	224	4.89	0.29	5.10	0.06	5.38	0.05	5.12
TZ - 3YB	1550/2	12007	103	4.89	0.05	5.14	0.03	5.40	0.03	5.14
TZ - 3YB	1550/5	11970	113	5.06	0.07	5.23	0.05	5.45	0.06	5.25
TZ - 3YB	1550/10	11738	127	5.53	0.13	5.41	0.07	5.62	0.07	5.52
TZ - 3YB	1600/2	11858	363	5.15	0.16	5.29	0.07	5.57	0.04	5.34
TZ - 3YB	1600/5	11849	551	5.80	0.21	5.43	0.05	5.62	0.04	5.62
TZ - 3YB	1600/10	11588	176	6.39	0.09	5.53	0.03	5.72	0.03	5.88
TZ - 3YB	1650/10	11361	293	6.75	0.21	5.82	0.12	5.87	0.06	6.15
TZ - 3YB	1650/20	11145	341	7.11	0.12	6.52	0.10	6.09	0.06	6.57
TZ - 3YB	1650/30	10971	293	7.94	0.24	7.50	0.54	7.80	0.15	7.77
B 261	1100/4	12867	789	4.89	0.08	5.35	0.14	-	-	5.12
B 261	1300/6	12485	218	4.79	0.07	5.15	0.12	5.38	0.08	5.11
B 261	1450/2	10587	657	4.73	0.09	5.30	0.27	-	-	5.02
B 261	1550/5	10080	435	5.98	0.45	5.79	0.21	5.99	0.40	5.92

Recently Vickers indentation fracture toughness tests (VIF) were reviewed in detail [22]. It was concluded that VIF techniques are not suitable for reliable measurement of fracture toughness, K_{Ic}, because the crack arrest process occurs in a multiple-crack environment and in highly complex residual stress conditions. To verify our fracture toughness results determined by the indentation method, two standardized methods were applied. Unfortunately, the results obtained by "Chevron V Notch" method (CVN) and "Single Edged V Notch Beam" method (SEVNB) showed extremely high scatter (5-12 MPam$^{0.5}$), thus it was not possible to find any dependence on grain size. The reason for such high variance is not clear and may be connected with the toughening effect in TZP ceramics. From this point of view the indentation method utilized in the present investigation provided more consistent results compared with the CVN and SEVNB methods.
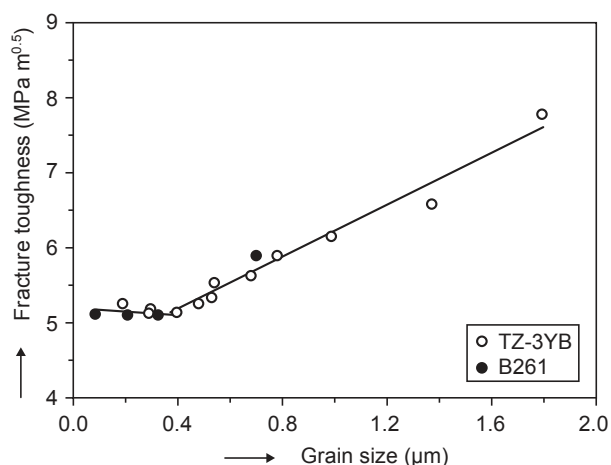

Figure 9. Average fracture toughness of TZ-3YB and B261 ceramics as a function of grain size.
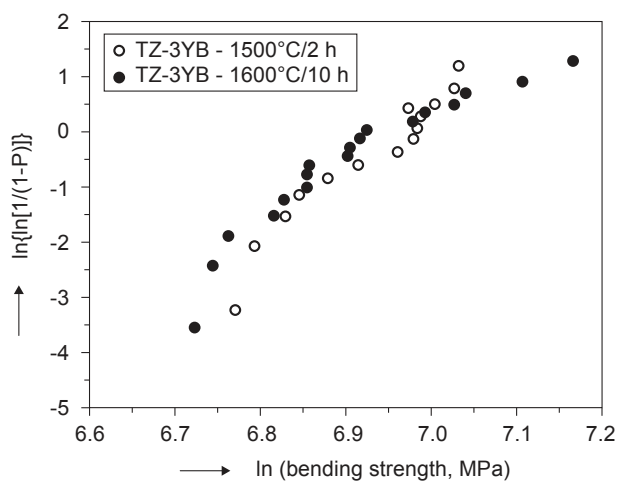

Figure 10. Weibull plot of the bending strength data for TZ-3YB ceramics sintered at 1500°C for 2 h and at 1600°C for 10 h.

The four-point bending strength of TZ-3YB bars with a grain size of 0.30 μm (sintered at 1500°C/2 h) and 0.78 μm (sintered at 1600°C/10 h) was determined and compared. Figure 10 shows the Weibull plot of both materials. Although the average strength of samples varying in grain size was similar (1020 MPa vs. 1011 MPa), it can be seen in the graph that the scatter of strength values was higher for TZ-3YB ceramics with larger grains. This observation was confirmed by calculation of Weibull moduli. The Weibull modulus was $m = 13.0$ for ceramics with the grain size of 0.30 μm and $m = 7.54$ for ceramics with the grain size of 0.78 μm. It was verified statistically that these values are significantly different. According to the linear fracture mechanics the body with higher fracture toughness should possess the higher strength. In our case TZ-3YB ceramics with a grain size of 0.78 μm had higher toughness than ceramics with a grain size of 0.30 μm (5.88 vs. 5.17 MPam$^{0.5}$). Unfortunately, the effect of higher toughness was suppressed by an effect of bigger critical defects due to microstructural coarsening [10]. The competition of these two effects resulted in ceramics with strengths apparently independent of grain size. However, the size and distribution of defects during coarsening cannot be efficiently controlled, which resulted in the lower Weibull modulus for ceramics sintered at higher temperature.

CONCLUSION

The effect of grain size on mechanical properties of commercial submicrometre-grained 3Y-TZP ceramics (TZ-3YB) and nanocrystalline 3Y-zirconia ceramics (B261) was investigated. The following conclusions could be drawn:

1. The hardness of both TZ-3YB and B261 ceramics decreased with increasing grain size. However, the hardness was lower in coarsened nanoceramics. This could be attributed to different mechanisms of the development of phase structure in nanoceramics compared with submicrometre-grained ceramics.

2. The fracture toughness was almost constant (5.1 MPam$^{0.5}$) up to the grain size of 0.4 μm. Above this grain size, the fracture toughness started to grow and reached the maximum of 7.8 MPam$^{0.5}$ at the grain size of 1.8 μm. Further grain growth resulted in spontaneous transformation from tetragonal to monoclinic phase and damage of the samples due to cracking. Both ceramics followed the same grain size depen-dence of fracture toughness.

3. The four-point bending strength of TZ-3YB ceramics with grain size of 0.30 and 0.78 μm was similar, 1020 MPa and 1011 MPa, respectively. The higher

fracture toughness inherent to ceramics with larger grain size was counterbalanced with an increase of critical defects due to microstructural coarsening. Moreover, the Weibull modulus declined from $m = 13$ at a grain size of 0.30 μm to $m = 7.54$ at a grain size of 0.78 μm.

Acknowledgement

References

1. Hannink R. H. J., Kelly P. M., Muddle B. C.: J.Am.Ceram.Soc. *83*, 461 (2000).
2. Lange F. F.: J. Mater.Sci. *17*, 225 (1982).
3. Lange F. F.: J.Mater.Sci. *17*, 240 (1982).
4. Becher P. F., Swain M. V.: J.Am.Ceram.Soc. *75*, 493 (1992).
5. Wang J, Rainforth M., Stevens R.: Br.Ceram.Trans.J. *88*, 1 (1989).
6. Suresh A., Mayo M. J., Porter W. D., Rawn C. J.: J.Am.Ceram.Soc. *86*, 360 (2003).
7. Bravo-Leon A., Morikawa Y., Kawahara M., Mayo M. J.: Acta Mater. *50*, 4555 (2002).
8. Ruiz L., Readey M. J.: J.Am.Ceram.Soc. *79*, 2331 (1996).
9. Casellas D., Feder A., Llanes L., Anglada M.: Scr.Mater. *45*, 213 (2001).
10. Eichler J., Rödel J., Eisele U., Hoffman M.: J.Am.Ceram.Soc. *90*, 2830 (2007).
11. Casellas D., Alcala J., Llanes L., Anglada M.: J.Mater.Sci. *36*, 3011 (2001).
12. Cottom B. A., Mayo M. J.: Scr.Mater. *34*, 809 (1996).
13. Trunec M., Maca K.: J.Am.Ceram.Soc. *90*, 2735 (2007).
14. EN 623-2: Advanced Technical Ceramics - Monolithic Ceramics. General and Texture Properties. Part 2: *Determination of Density and Porosity*, CEN, Brussels 1993.
15. Maca K., Trunec M., Chmelik R.: Ceramics-Silikaty *51*, 94 (2007).
16. Niihara K., Morena R., Hasselman D. P. H.: J.Mater.Sci. Lett. *1*, 13 (1982).
17. JIS R 1607: *Testing Methods for Fracture Toughness of High Performance Ceramics*, Japanese Standards Association, Tokyo 1990.
18. EN 843-1: Advanced Technical Ceramics - Monolithic Ceramics. Mechanical Properties at Room Temperature. Part 1: *Determination of Flexural Strength*, CEN, Brussels 1995.
19. ENV 843-5: Advanced Technical Ceramics - Monolithic Ceramics. Mechanical Properties at Room Temperature. Part 5: *Statistical Analysis*, CEN, Brussels 1996.
20. Scott H. G.: J.Mater.Sci. *10*, 1527 (1975).
21. Matsui K., Horikoshi H., Ohmichi N., Ohgai M.: J.Am.Ceram.Soc. *86*, 1401 (2003).
22. Quinn G. D., Bradt R. C.: J.Am.Ceram.Soc. *90*, 673 (2007).

VLIV VELIKOSTI ZRN NA MECHANICKÉ
VLASTNOSTI 3Y-TZP KERAMIKY

MARTIN TRUNEC

Odbor keramiky a polymerů, Vysoké učení technické v Brně, Technická 2896/2, 616 69 Brno

Mechanické vlastnosti 3Y-TZP keramiky byly zkoumány v závislosti na velikosti zrn v rozsahu od 0,19 μm do 2,15 μm. Vickersovy indentační testy byly použity pro stanovení tvrdosti a lomové houževnatosti. Tvrdost klesala s rostoucí velikostí zrn. Lomová houževnatost byla téměř konstantní pro keramiky se zrny do 0,4 μm a poté rostla se zvyšující se velikosti zrn až na 7,8 MPam^{0,5} u keramiky se zrny o velikosti 1,8 μm. U větších zrn došlo ke spontánní transformaci tetragonální fáze na monoklinickou. Keramické vzorky s velikostí zrn 0,30 μm a 0,78 μm měli podobnou pevnost v ohybu, 1020 a 1011 MPa. Mikrostrukturní zhrubnutí, které bylo nezbytné pro dosažení větších zrn, vedlo k vyššímu rozptylu pevností, což se projevilo snížením Weibullova modulu (13,0 vs. 7,54). Pro srovnání byly také zkoumány mechanické vlastnosti nanokrystalické 3Y-ZrO$_2$ keramiky, jejíž zrna byla zhrublá na velikost od 0,085 do 0,70 μm. Byly zjištěny rozdíly v mechanických vlastnostech zkoumaných keramik. Možné příčiny těchto rozdílů byly diskutovány.